European Journal of Medicinal Chemistry 45 (2010) 4427–4434

Contents lists available at ScienceDirect

European Journal of Medicinal Chemistry

journal homepage: http://www.elsevier.com/locate/ejmech

Original article

Synthesis and CYP24A1 inhibitory activity of (*E*)-2-(2-substituted benzylidene)- and 2-(2-substituted benzyl)-6-methoxy-tetralones

Ahmed S. Aboraia [a,1], Bart Makowski [b], Alba Bahja [a], David Prosser [b], Andrea Brancale [a], Glenville Jones [b], Claire Simons [a,*]

[a] Medicinal Chemistry, Welsh School of Pharmacy, Cardiff University, King Edward VII Avenue, Cardiff CF10 3NB, UK
[b] Department of Biochemistry, Queens University, Kingston, Ontario, Canada K7L 3N6

ARTICLE INFO

Article history:
Received 12 February 2010
Received in revised form
20 May 2010
Accepted 1 July 2010
Available online 8 July 2010

Keywords:
Benzylidene tetralones
Benzyl tetralones
CYP24A1
CYP27A1
Enzyme inhibition
Molecular modelling

ABSTRACT

A series of (*E*)-2-(2-substituted benzylidene)- and 2-(2-substituted benzyl)-6-methoxy-tetralones were prepared, using an efficient synthetic scheme, and evaluated for their inhibitory activity against cytochrome P450C24A1 (CYP24A1) hydroxylase. In general the reduced benzyl tetralones were more active than the parent benzylidene tetralones. The 2-ethyl and 2-trifluoromethyl benzyl tetralone derivatives (**4c** and **4b**) showed optimal activity in this series with IC_{50} values of 1.92 μM and 2.08 μM, respectively compared with the standard ketoconazole IC_{50} 0.52 μM. The 2-bromobenzyl tetralone (**4d**) showed a preference for CYP27A1 (IC_{50} 59 nM) over CYP24A1 (IC50 16.3 μM) and may be a useful lead in CYP27A1 inhibition studies. The 2-ethylphenyl benzyl derivative (**9c**), which showed weak activity against the wild type CYP24A1 (IC_{50} 25.57 μM), exhibited enhanced inhibitory activity towards L148F and M416T mutants, this difference in activity for the L148F mutant has been explained using molecular modelling.

1. Introduction

Vitamin D_3 is converted to 25-hydroxycholecalciferol or calcidiol in the liver, and then metabolised by the kidney to the active form 1α,25-dihydroxycholecalciferol (1α,25$(OH)_2D_3$) or calcitriol (Fig. 1) [1]. Calcitriol then binds to the vitamin D receptor (VDR), which mediates tissue-specific effects including enhancement of intestinal calcium transport, maintenance of skeletal health and epidermal integrity and immune cell regulation. Replacement calcitriol therapy has been used in chronic kidney disease, hyperproliferative skin diseases and osteoporosis, with clinical trials for various forms of cancer and autoimmune conditions ongoing [2].

Although the potential of vitamin D as an antiproliferative drug has been realised in psoriasis and parathyroid cell hyperplasia, an anticancer treatment incorporating vitamin D remains a challenge owing to increased drug resistance. Evidence is growing that this resistance is caused by upregulation of the cytochrome P450 enzyme, CYP24A1, resulting in accelerated metabolism of calcitriol and derivatives [1,3]. Inhibitors of CYP24A1 are expected to extend the t1/2 of calcitriol thereby enhancing endogenous levels of calcitriol, or vitamin D analogues, which may result in stabilised CYP24A1 and enhanced stability of vitamin D compounds.

The challenge in the design of CYP24A1 inhibitors is designing selective CYP24A1 inhibitors with respect to other CYPs including CYP27A1 and CYP27B1.

CYP inhibitors fall in to two main categories, azole and non-azole inhibitors. Azole inhibitors have a nitrogen heterocyclic ring, commonly an imidazole or triazole, within the structure and it is through a nitrogen of the heterocyclic ring that binding occurs with the Fe^{3+} of the haem. Non-azole inhibitors lack this nitrogen heterocycle with binding within the active site involving hydrogen bonding and hydrophobic interactions, however the strength of these interactions are usually less than that observed with azole inhibitors resulting in less potent inhibitors. However, the potential benefit of non-azole inhibitors is greater selectivity against other CYP enzymes compared with azole inhibitors, which makes non-azole inhibitors a valid area to explore.

Ketoconazole, a broad spectrum CYP inhibitor is an azole compound with CYP24A1 inhibitory activity and approximately 4-fold selectivity for CYP24A1 *vs* CYP27B1 [4]. Schuster et al. [4] described the azole compound (*R*)-VID400 (Fig. 2), which displayed a 40-fold selectivity for CYP24A1 over CYP27B1. Calcitriol

* Corresponding author. Tel.: +44 2920 876307; fax: +44 2920 874149.
E-mail address: simonsc@cardiff.ac.uk (C. Simons).
URL: http://www.cardiff.ac.uk/phrmy/staffinfo/cs/homepage/cs.html
[1] Present address: Medicinal Chemistry Department, Faculty of Pharmacy, Assiut University, Assiut, Egypt.

0223-5234/$ – see front matter © 2010 Elsevier Masson SAS. All rights reserved.
doi:10.1016/j.ejmech.2010.07.001

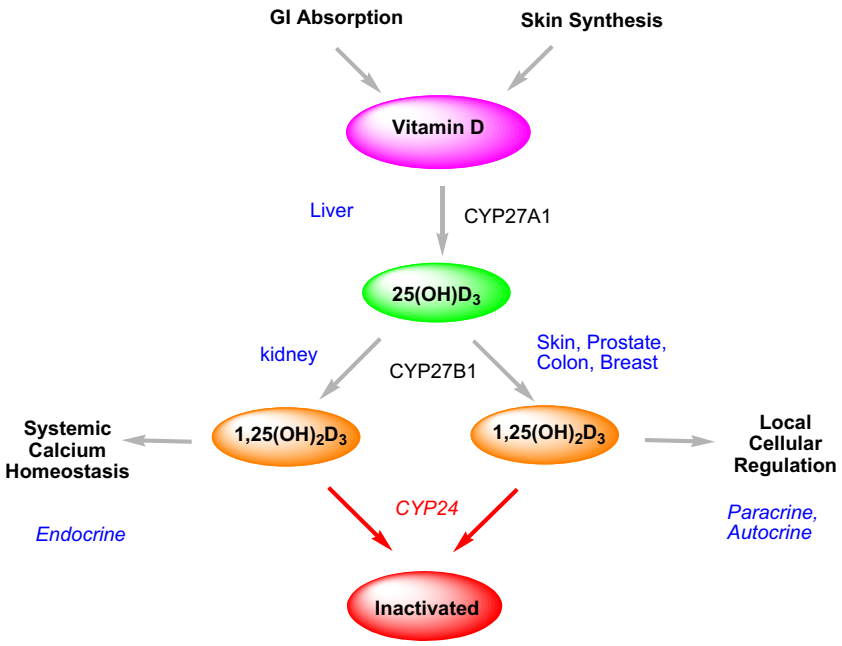

Fig. 1. The active form of Vitamin D (calcitriol/1α,25-$(OH)_2D_3$) interacts with the VDR in an endocrine or autocrine fashion.

derivatives with sulfoximine modification of the 24-hydroxy group (Fig. 2) resulted in compounds with CYP24A1 selectivity (75-fold selectivity CYP24A1/CYP27B1) and low calcemic activity, determined using an *in vivo* rat model [5].

The effects of CYP24 inhibitors at a molecular level with non-azole compounds have been described by two groups. At Cardiff [6] novel tetralone CYP24A1 inhibitors, combined with calcitriol, displayed enhanced antiproliferative activity in DU145 cells and upregulation of VDR genes *CYP24A1*, $p21^{waf1/cip1}$ and *GADD45a* (Fig. 2). Swaimi et al. [7] studied the phytoestrogen genestein, which, in combination with calcitriol, increased the t1/2 of calcitriol and VDR levels resulting in significant enhancement of calcitriol-mediated functional responses including upregulation of mRNA levels of p21/WAF1, p21 and IGFBP-3 gene.

We have previously described a series of 2-substituted-3,4-dihydro-2*H*-naphthalen-1-one (tetralone) derivatives with promising CYP24 inhibitory activity in a rat kidney mitochondrial assay, compared with the standard ketoconazole (IC_{50} = 20 μM) [8]. The most potent tetralones were the 2-methyl and 2-phenyl-substituted benzyl tetralones with IC_{50} values of 0.9 and 2.1 μM respectively (Fig. 3). This paper describes the further development of these lead compounds to explore the effect of varying the 2-substituents on IC_{50}. A slight preference for a 6-methoxy rather than a 6-hydroxy substituent in the naphthalene ring was noted; therefore the 6-methoxy has been included.

The benzylidene tetralones were found to be very poor inhibitors in the rat kidney mitochondrial assay compared with the saturated benzyl tetralones [8], this was in contrast to previous studies with benzylidene 2-(pyridylmethylene)-1-tetralones which showed potent inhibitory activity against aromatase (CYP19) [9]. As a cell based CYP24A1 assay using Chinese hamster lung fibroblasts (V79-4) stably expressing CYP24A1 was employed in this research [10], both the benzylidene precursors and final benzyl derivatives (Fig. 1) were evaluated, to determine any differences (species and mitochondrial *versus* cell). For some of the compounds selectivity was assessed by determining the inhibitory activity against CYP27A1, and a preliminary study to investigate the inhibitory activity against mutant CYP24A1 strains was also performed.

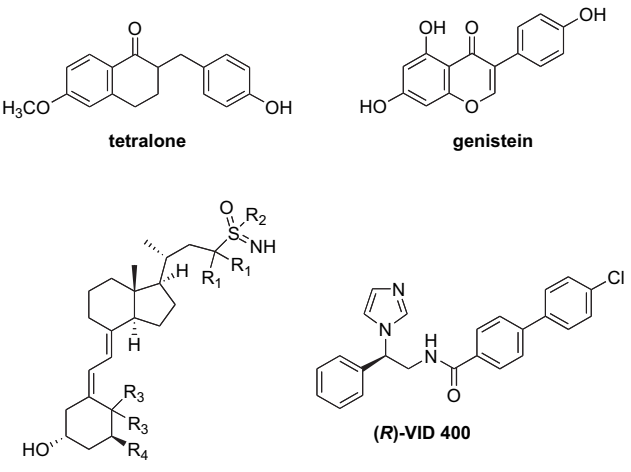

Fig. 2. Described CYP24A1 inhibitors.

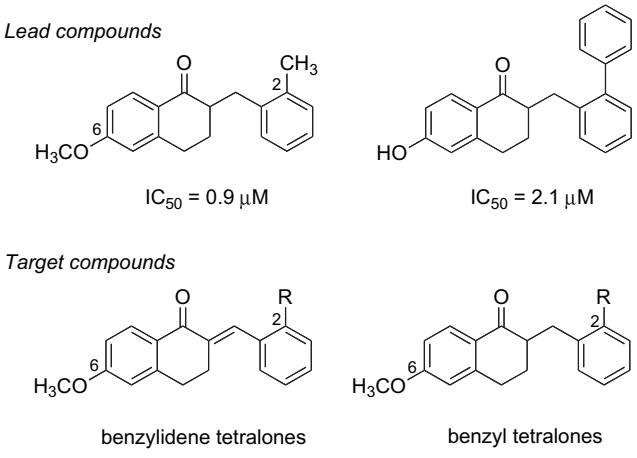

Fig. 3. Lead and target 2-substituted tetralone derivatives.

Docking experiments were performed to rationalise some of the data obtained.

2. Results and discussion

2.1. Chemistry

All the syntheses of the tetralone derivatives were performed by the general methods outlined in Schemes 1 and 2. The synthesis was based on the procedure described by our group [8,11].

The method employed for the preparation of the (*E*)-2-(2-substituted benzylidene)-6-methoxytetralone derivatives (**3a**–**c**) involved direct condensation of commercially available tetralone (**1**) with the appropriate benzaldehyde (**2**) in ethanolic KOH solution (Scheme 1) [12]. The reduced 2-(benzyl)-tetralones (**4a**–**c**) were readily obtained by hydrogenation with 10% Pd/C catalyst for 1 h, at approximately 30 psi (Parr hydrogenator) (Scheme 1). Preparation of the bromo derivative **4d** followed a three-step procedure involving first the preparation of the ethyl carboxylate (**5**) by reaction of 6-methoxy-1-tetralone (**1**) with NaH to abstract the acidic α-proton of the tetralone, and subsequent nucleophilic reaction of the carbanion with diethyl carbonate. Introduction of the bromophenyl used NaH to again abstract the acidic α-proton of the tetralone (**5**) followed by reaction with 2-bromobenzyl bromide. Decarboxylation of (**6**) was achieved on reaction with HBr and acetic acid to give the required 2-bromobenzyl tetralone (**4d**), however only in 29% yield (Scheme 1). The low yield resulted from demethylation of the 6-methoxy group, however this by-product was quantitatively converted to the required methoxy product (**4d**) on reaction with potassium carbonate and methyl iodide.

The 6-aryl substituted benzylidene derivatives (**8a** and **8b**) were prepared by Suzuki coupling of the 2-bromo-benzylidene tetralone (**7**) [8] with arylboronic acid in the presence of $Pd(PPh_3)_4$ catalyst (Scheme 2) [13]. Reduction of **8a** and **8b** by hydrogenation with 10% Pd/C catalyst for 1 h, at approximately 30 psi (Parr hydrogenator), gave the reduced 2-(benzyl)-tetralones (**9a**) and (**9c**). The 2-styrylbenzyl tetralone (**9b**) was prepared from **4d** by Suzuki coupling as described for the 2-aryl benzylidene derivatives **8a** and **8b**.

2.2. Biological results

Tetralones **3**, **4**, **7**, **8** and **9** were tested at 6 h incubation times on the wild type CYP24A1 expressing cell line. None of the inhibitors were more potent than ketoconazole (average $IC_{50} = 0.52$ μM). The IC_{50} values for the tetralones are summarised in Table 1, with the 2-ethyl-substituted benzyl tetralone **4c** having the highest potency with an IC_{50} of 1.92 μM. A preliminary docking of the inhibitors reported here was performed using PLANTS [14] and a homology model of CYP24A1 [15], shown in Fig. 4.

An assay assessing selectivity using the CYP27A1 cell line was performed and the IC_{50} values from these assays are summarised in Table 2. A preliminary assay assessing the inhibitory effect of some of the inhibitors on mutants of CYP24A1 is shown in Fig. 5.

2.2.1. CYP24A1 inhibitory data

Pairs of inhibitor structures e.g. **3** and **4**, show a systematic variation between a double and a single bond at the position of attachment between the tetralone and benzyl ring. The inclusion of a double bond at this position appeared to reduce the inhibitory effect in the inhibitors, which is consistent with our previous study [8]. For example, **4c** ($IC_{50} = 1.92$ μM) was more potent than its double bond counterpart, **3c** ($IC_{50} = 10.76$ μM) (Table 1). The double bond conjugates with the adjacent phenyl group resulting in decreased conformational flexibility of the structure.

This loss of flexibility could inhibit the entrance of the inhibitor through the access channel of CYP24A1, thus decreasing its access to the enzyme cavity where it would exert its inhibitory effect. Alternatively, the loss of conformational flexibility could prevent a favourable conformation that stabilises the inhibitor inside the enzyme cavity. Using a homology model of CYP24A1 [16] a molecular docking was performed using PLANTS [14], and single bond variants were found to have the capability of occupying the hydrophobic region on the enzyme cavity defined by Leu148, Ile242 and Val391 (Fig. 4), while the oxygen atom of the methoxy group is coordinating the haem iron. Furthermore, the phenyl moiety in the *S*-enantiomers establishes another series of interactions with Trp134, Pro392 and Ile149. Such hydrophobic interactions could stabilise the inhibitor conformation within the enzyme, thus increasing the inhibition capacity. It should be noted that both the *R*-enantiomer of compounds **4** and the double bonds derivatives (**3**) did not dock with the methoxy group coordinated with the haem-Fe and these results were not considered for further examination.

The two most potent inhibitors had an ethyl (**4c**) and a trifluoromethyl (**4d**) at the 2-position. When the 2-position is substituted with a methyl (**4a**) or a phenyl (**9a**) group, the inhibitory activity decreases (IC_{50} 126.9 μM and 127.6 μM respectively). Such

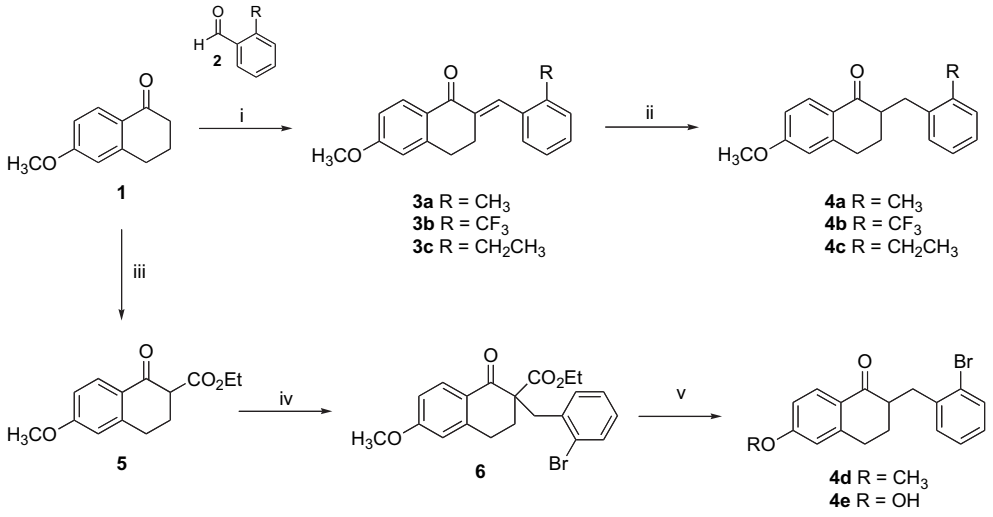

Scheme 1. *Reagents and conditions*: (i) 4% ethanolic KOH, 2–72 h (ii) 10% Pd/C, H_2, methanol, 30 psi,1 h (iii) NaH, diethyl carbonate, toluee, reflux, 18 h (iv) NaH, 2-bromobenzyl bromide, DMF, 60 °C, 8 h (v) HBr, AcOH, 120 °C, 1.5 h.

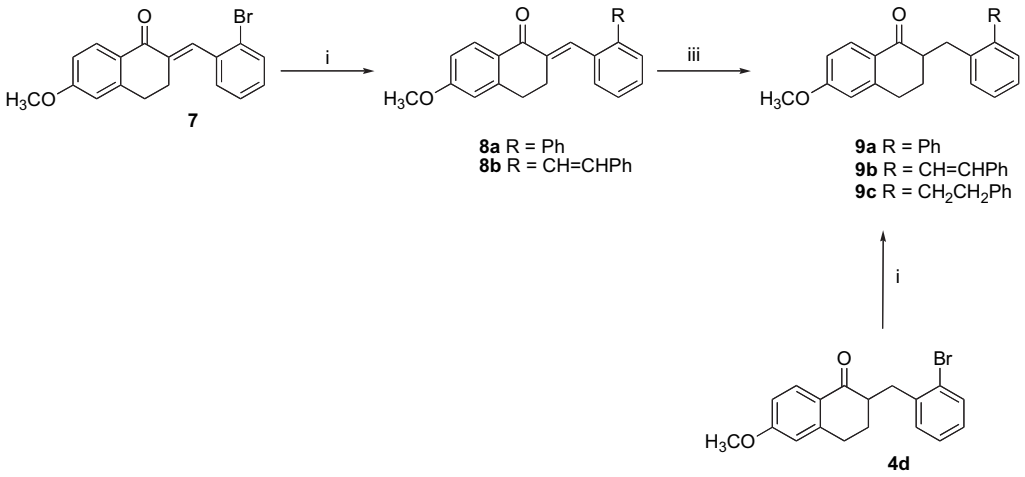

Scheme 2. *Reagents and conditions*: (i) (a) Arylboronic acid, $Pd(PPh_3)_4$, toluene, 100 °C, 5 h (b) H_2O_2, room temperature, 1 h (ii) 10% Pd/C, H_2, methanol, 1 atm,1 h (iii) 10% Pd/C, H_2, methanol, 30 psi,1 h.

a result could indicate that the ethyl group has a stabilising effect on the binding of the inhibitor, but unfortunately the docking studies are inconclusive on this matter and it is not possible to identify a specific structural justification to the observed activity profile.

The strong inhibitory capacity of **4b** could reflect a trend observed in inhibitor design; the addition of fluorine groups increases the inhibitory capacity of a compound. It has been suggested that this increase is not caused by a stronger enzyme–inhibitor complex, but by increasing the cell-membrane penetrating capacity and thus increasing the bioavailability. However, many of the compounds appear to be hydrophobic and should have little problem penetrating cell membranes. As such, the fluorination may have a stabilising effect on the inhibitor inside the enzyme resulting in more effective inhibition.

2.2.2. CYP27A1 assay

A potent and specific inhibitor of CYP24A1 would display a low IC_{50} value towards CYP24A1 and a high IC_{50} value towards related cytochrome P450s. CYP27A1 is a good enzyme to test for specificity because of its structural similarity to CYP24A1, as well as the structural similarity of their respective substrates (1α-OH-D_3 and 1α,25-$(OH)_2D_3$).

Upon comparison of IC_{50} values between CYP24A1 and CYP27A1 (Table 2), it is clear that none of the most potent tetralone inhibitors of CYP24A1 are particularly specific, i.e. they have similar IC_{50} values for CYP27A1. Surprisingly, the 2-bromo-substituted benzyl tetralone (**4d**) displayed a much greater potency towards CYP27A1 than CYP24A1 (276-fold selectivity), likewise the 2-bromo-substituted benzylidene tetralone (**7**), although considerably less potent, displayed a 28-fold selectivity towards CYP27A1 (Table 2); such an outlier could be quite useful in future inhibition studies of CYP27A1.

Table 1
CYP24A1 inhibitory (IC_{50}) data for the tetralone derivatives.

No.	R	IC_{50} (μM)[a]	No.	R	IC_{50} (μM)[a]
	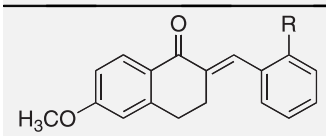			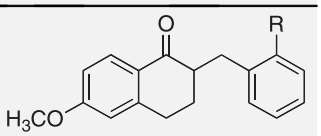	
3a	CH_3	480.1	**4a**	CH_3	126.9
3b	CF_3	11.22	**4b**	CF_3	2.08
3c	CH_2CH_3	10.76	**4c**	CH_2CH_3	1.92
7	Br	122.0	**4d**	Br	16.3
8a	Ph	111.1	**9a**	Ph	127.6
8b	CH=CHPh	5.08	**9b**	CH=CHPh	342.8
			9c	CH_2CH_2Ph	25.57

[a] IC_{50} values are the average (±5%) of two experiments. Ketoconazole (IC_{50} 0.52 μM) was used as the standard for comparison.

2.2.3. Mutant studies

A preliminary assay was performed to screen for the possibility of a mutated residue causing a weak inhibitor to be more potent. It was found that the 2-phenylethyl-substituted benzyl tetralone (**9c**) was significantly more potent towards two mutants relative to the wild type form of the enzyme (L148F and M416T) (Fig. 5). L148F is a mutant strain characterised by a shift towards C24 metabolism, coupled with an increase in calcitroic acid metabolism. The Leu148 residue is located in the hydrophobic pocket described earlier that

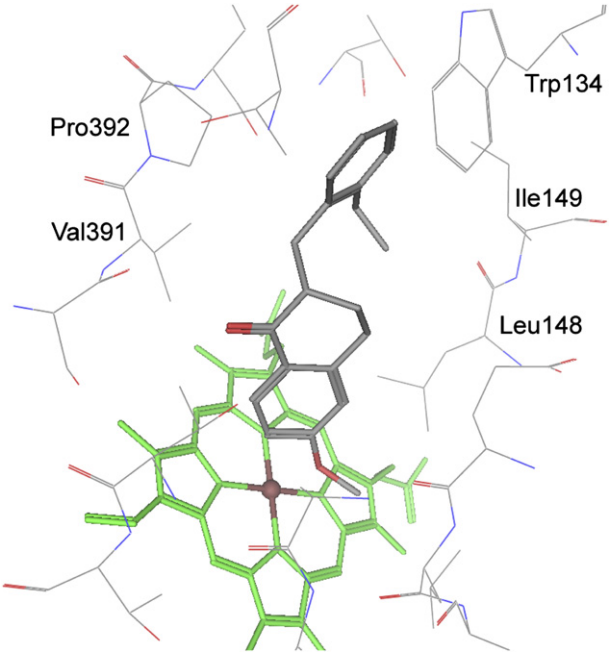

Fig. 4. Preliminary Docking of **4c** into the CYP24A1 Homology Model Enzyme Cavity. The phenyl group is able to occupy the hydrophobic region within the cavity. This cavity is proximal to the hydrophobic residues Leu148, Ile 131 and Leu 129.

Table 2
CYP24A1 and CYP27A1 IC_{50} data for the tetralone derivatives.

Tetralone	IC_{50} (μM)[a] CYP27A1	IC_{50} (μM)[a] CYP24A1
7	4.33	122.0
4d	0.059	16.3
4b	5.34	2.08
4c	8.23	1.92
8b	5.69	5.08

[a] IC_{50} values are the average (±5%) of two experiments.

could be responsible for inhibitor stabilization. In a wild-type setting the Leu148 residue is thought to interact with the A-ring of $1\alpha,25\text{-}(OH)_2D_3$ [15].

To investigate the increase in activity of **9c** in the L148F mutant, we have introduced the appropriate mutations in our model using the rotamer explorer function in MOE [17]. From the docking results of **9c** it is possible to observe (Fig. 6) that the phenylalanine side chain could establish a π–π interaction with the aromatic ring connected to the tetralone scaffold (in the *S*-configuration), leading to an increased binding affinity of this compound in this specific mutant.

The M416T mutant also shows increased calcitroic acid production capabilities, however the residue is thought to be located near the access channel and in our model, it is just in contact with the terminal aromatic ring of **9c**. In this case, the model with the appropriate mutation does not show a clear structural advantage for the binding of this analogue, as with the previous mutant. It is possible that the bulkier tetralone **9c** (relative to the other tetralones) might have a higher inhibitory capacity with respect to this mutant because of a wider access channel. As a result, **9c** may be able to access the CYP24A1 enzyme cavity with greater ease and allow the interaction of its bulky R group with the internal residues of the cavity.

There appears to be an anomaly with the 2-phenyl-substituted benzylidene (**8a**) and benzyl (**9a**) tetralones in that they do not inhibit CYP24A1 activity in this assay. This could be a result of these two inhibitors being so poor that the initial IC_{50} values were actually a reflection of the decrease in cell viability and not of their inhibitory capacity. In the CYP24A1 assays, a large amount of ethanol was used at the 10^{-4} M data point (~50 μL/mL of medium) because the inhibitor needed 1 mL of ethanol to dissolve 1 mg. This may have led to a lower apparent IC_{50} value that was not carried through in the mutant experiment.

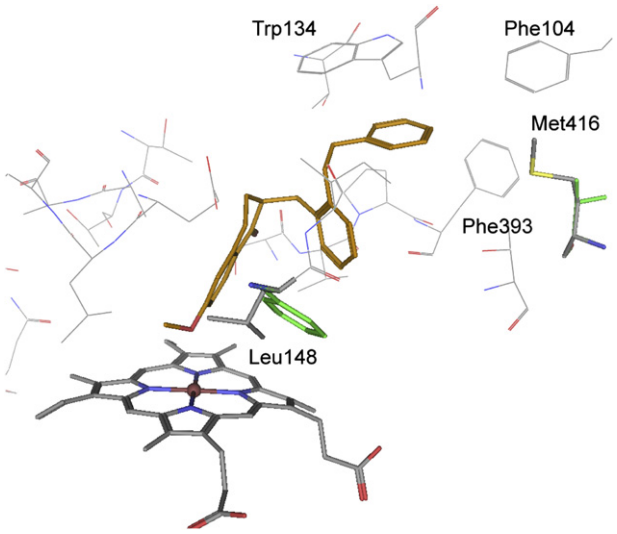

Fig. 6. Docking of **9c** into the 'mutated' L148F CYP24A1 Homology Model Enzyme Cavity.

3. Conclusions

The most potent benzyl tetralones displayed moderate CYP24A1 inhibitory activity in the described assay. Very different results were obtained for the 2-methyl substituted benzyl tetralone (Fig. 3, **4a**), with the promising CYP24A1 inhibitory activity (IC_{50} 0.9 μM) compared with ketoconazole (IC_{50} 20 μM) previously seen in the rat microsomal assay [8], not translating to the cell based assay employed here (**4a** IC_{50} 126.9 μM; ketoconazole IC_{50} 0.52 μM), suggesting than the enzyme active site cavity in rat is probably different enough to affect IC_{50}, this is perhaps supported by the mutant study performed here with one amino acid mutation resulting in notable differences in inhibitory activity (Fig. 5).

The inhibition of CYP24A1 by tetralones is still not as well characterised as that of azole-based inhibitors, however with the information gained from the docking and mutant experiments, it may be possible to refine the compounds to increase the potency and/or specificity of this class of inhibitors. The use of tetralones to inhibit CYP24A1 may have unforeseen advantages over some of the current published inhibitors, and it is worthwhile to pursue future generations of such inhibitors. Not only could such inhibitors be

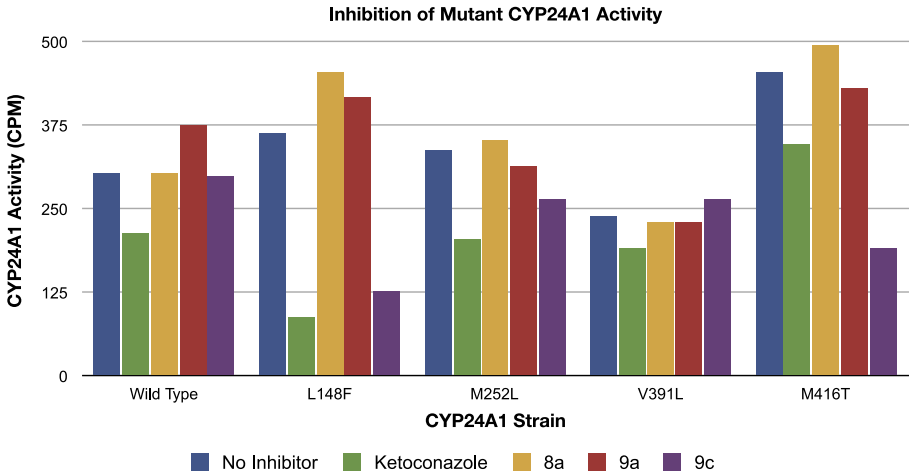

Fig. 5. Inhibitor Capacity of Weak Novel Inhibitors on CYP24A1 Mutant Strains. An anomaly is apparent with MCC 179 (**8a**) and MCC180 (**9a**) where the activity is higher than the non-inhibited wild type. The interesting result comes from an increase in potency of ketoconazole and **9c** (MCC 183) towards L148F and M416T mutants.

useful in a clinical setting, but they could also advance the understanding of the structure and binding mechanism of CYP24A1.

4. Experimental

4.1. Pharmacology

4.1.1. CYP24A1and CYP27A1 preparation and assay

Cell culture: Chinese hamster lung fibroblasts (V79-4) stably expressing either CYP24A1 (WT, L148F, M252L, V391L, or M416T) [10] or CYP27A1 (WT) [16] were maintained and grown using Dulbecco's Modified Eagle Medium (DMEM) purchased from Invitrogen Life Technologies. The growth medium was supplemented with fetal calf serum (FCS) as well as antibiotics (1% v/v) and hygromycin (0.2% v/v) and glucose (1 g/500 mL). Cells were plated on standard 100 mm cell culture dishes and were maintained in a humidified atmosphere of 5% CO_2 in air.

Inhibitor preparations: Milligram quantities of the inhibitors were dissolved in 100% ethanol, while ketoconazole was dissolved in 0.05 M HCl. A 1 mg/mL stock solution was made up for each inhibitor to be tested. Serial 1/10 dilutions were then made to give stock solutions suitable for the low concentration incubations.

Incubations: Prior to incubation, cells were grown on P-150 plates until reaching ~100% confluence. The cells were then subcultured onto 6-well plates in the FCS-supplemented DMEM for 24 h. The incubation medium for the experiments was BSA supplemented (1% w/v) DMEM containing the appropriate substrate; 100,000 CPM per well of [1β-^{3}H]1α,25-$(OH)_2D_3$ for the CYP24A1-containing cells and 10 μM 1α-OH-D_3 for the CYP27A1-containing cells. Each well also contained 1 μL of DPPD (100 μM) to act as an anti-oxidant. Each assay was conducted with a 'no inhibitor', 'dead cell' and 'no cell' control. The 'dead cell' control was prepared by microwaving the plate of cells for 30 s prior to incubation and each well contained 1 mL of incubation medium. Each inhibitor was tested at 4 different concentrations; 1×10^{-4} M, 1×10^{-5} M, 1×10^{-6} M, and 1×10^{-7} M. The CYP24A1 assays were carried out at an optimized 6 h time interval, while the CYP27A1 assay was carried out at a 24 h interval which had been previously optimized. The incubations were arrested by the addition of 2.5 mL of methanol to each well.

Extraction: The incubation medium was extracted using a modified Bligh and Dyer extraction [16]. For samples destined for HPLC analysis (mainly samples taken from CYP27A1 assays), 2 μg of 25-OH-D_3 was added to each sample as an internal recovery standard for subsequent normalization of metabolite quantification. The samples from the CYP24A1 assays were analysed using scintillation counting of 0.5 mL of the aqueous phase (from the Bligh and Dyer extraction). Beckman Coulter Ready Safe™ Liquid Scintillation Cocktail for Aqueous Samples (5 mL) was added to the 0.5 mL samples, and scintillation counting was performed using a Beckman Coulter L6500 Multipurpose Scintillation Counter.

High performance liquid chromatography: To determine the amount of metabolite formed in the CYP27A1 incubations, HPLC paired with a photodiode array detector (Waters 996 PDA) or a RadioFlow Detector (LB509; EG&G Berthold, Bad Wilbad, Germany) was used. The HPLC uses a Zorbax-Sil column (3 μm; 6.2 × 80 mm) coupled to a Waters 1695 Separation Module, and a solvent system of 91% hexane (v/v), 7% isopropanol (v/v), 2% methanol (v/v) at a flow rate of 1.0 mL/min for a 30 min run time. The organic phase of the Bligh and Dyer extraction was dried down under N_2 gas, dried with 400 μL of ethanol, and then prepared in 110 μL of HPLC solvent. Empower software (Waters Corp.) was used to integrate the peaks and determine the amount of metabolite formed (ng) by analysing the peaks characteristic for vitamin D ($\lambda_{max} = 265$ nm, $\lambda_{min} = 228$ nm, and $\varepsilon = 18{,}300$).

4.2. Chemistry

^{1}H and ^{13}C NMR spectra were recorded with a Brucker Avance DPX500 spectrometer operating at 500 and 125 MHz, with Me_4Si as internal standard. Mass spectra were determined by the EPSRC mass spectrometry centre (Swansea, UK). Microanalyses were determined by Medac Ltd (Surrey, UK). Flash column chromatography was performed with silica gel 60 (230–400 mesh) (Merck) and TLC was carried out on precoated silica plates (kiesel gel 60 F_{254}, BDH). Melting points were determined on an electrothermal instrument and are uncorrected. Compounds were visualised by illumination under UV light (254 nm) or by the use of vanillin stain followed by charring on a hotplate. All solvents were dried prior to use as-described by the handbook Purification of Laboratory Chemicals [18] and stored over 4 Å molecular sieves, under nitrogen. We have previously described compounds **3a**, **4a**, **5**, **7a** and **8a** [8,19]. Compound **5** was prepared according to the literature method [20].

The numbering of compounds for NMR characterisation is as follows:

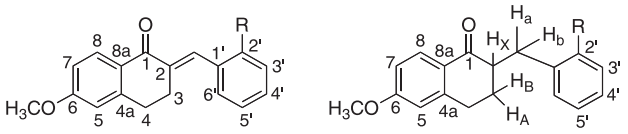

4.2.1. General procedure for the synthesis of (E)-2-(2-substituted benzylidene)-6-methoxy-tetralone derivatives (**3**)

A mixture of the 6-methoxytetralone (**1**) (2.0 g, 11 mmol) and 2-substituted benzaldehyde (**2**) (11 mmol) in 4% ethanolic KOH (100 mL) was stirred at room temperature for 1 h. The resulting precipitate was collected, washed with water and finally recrystallised from ethanol.

*4.2.1.1. (E)-2-(2-Trifluoromethylbenzylidene)-6-methoxy-tetralone (**3b**).* A cream crystalline solid was obtained. Yield: 2.48 g (68%), R_f 0.54 (petroleum ether–EtOAc 3:1 v/v); m.p. 81–83 °C; ^{1}H NMR: δ 8.17 (d, $J = 8.8$ Hz, 1H, H-8), 7.96 (s, 1H, –C=CH-Ph), 7.75 (d, $J = 7.9$ Hz, 1H, H-3′), 7.58 (t, $J = 7.6$ Hz, 1H, H-6′), 7.47 (t, $J = 7.7$ Hz, 1H, H-5′), 7.34 (d, $J = 7.6$ Hz, 1H, H-4′), 6.91 (dd, $J = 2.5$, 8.8 Hz, 1H, H-7), 6.72 (d, $J = 2.4$ Hz, 1H, H-5), 3.89 (s, 3H, OCH_3), 2.91 (m, 2H, CH_2), 2.85 (m, 2H, CH_2). ^{13}C NMR: δ 189.2 (C, C=O), 163.8 (C, C-6), 146.0 (C), 138.2 (C), 135.2 (C), 132.3 (CH), 131.5 (CH), 130.9 (CH), 130.4 (CH), 129.34 (C, C–F), 129.1 (C, C–F), 127.9 (CH), 126.8 (C), 126.1 (CH), 125.0 (C), 122.9 (C, C–F), 113.5 (CH), 112.4 (CH), 55.5 (CH_3), 29.5 (CH_2), 27.4 (CH_2). Anal. Calcd. for $C_{19}H_{15}O_2F_3 \cdot 0.1H_2O$ (334.123): C, 68.30%, H, 4.59%. Found: C, 68.24%, H, 4.45%.

*4.2.1.2. (E)-2-(2-Ethylbenzylidene)-6-methoxy-tetralone (**3c**).* A light yellow crystalline solid was obtained. Yield: 2.33 g (72%), R_f 0.74 (petroleum ether–EtOAc 3:1 v/v); m.p. 78–80 °C; ^{1}H NMR: δ 8.18 (d, $J = 8.7$ Hz, 1H, H-8), 7.97 (s, 1H, –C=CH-Ph), 7.27 (m, 4H, Ar), 6.91 (dd, $J = 2.5$, 8.8 Hz, 1H, H-7), 6.73 (d, $J = 2.4$ Hz, 1H, H-5), 3.90 (s, 3H, OCH_3), 2.97 (m, 2H, CH_2), 2.91 (m, 2H, CH_2), 2.72 (q, $J = 7.6$ Hz, 2H, CH_2CH_3), 1.21 (t, $J = 7.6$ Hz, 3H, CH_2CH_3). ^{13}C NMR: δ 186.8 (C, C=O), 163.6 (C, C-6), 146.0 (C), 143.8 (C), 136.4 (C), 135.0 (CH), 134.6 (C), 130.8 (CH), 129.1 (CH), 128.5 (CH), 127.1 (C), 125.5 (CH), 113.4 (CH), 112.4 (CH), 55.5 (CH_3), 29.7 (CH_2), 27.3 (CH_2), 26.7 (CH_2CH_3), 15.1 (CH_2CH_3). Anal. Calcd. for $C_{20}H_{20}O_2$ (292.377): C, 82.16%, H, 6.89%. Found: C, 82.25%, H, 7.15%.

4.2.2. General procedure for the synthesis of 2-(2-substituted benzyl)-6-methoxy-tetralone derivatives (**4** and **9c**)

A mixture of the (*E*)-2-(2-substituted benzylidene)-6-methoxy-tetralone (**3** or **8b**) (2.0 g, 6 mmol) and 10% Pd on charcoal (160 mg) in methanol (200 mL), was shaken in an atmosphere of hydrogen at

room temperature for 1 h. Pd was removed by filtration over a bed of celite and the filtrate was concentrated *in vacuo* to give a yellow residue. Purification by flash column chromatography (petroleum ether–EtOAc 90:10 v/v) gave the product.

*4.2.2.1. 2-(2-Trifluoromethylbenzyl)-6-methoxy-tetralone (**4b**).* A cream crystalline solid was obtained. Yield: 1.03 g (53%), R_f 0.60 (petroleum ether–EtOAc 3:1 v/v); m.p. 82–84 °C; ^{1}H NMR: δ 8.08 (d, J = 8.8 Hz, 1H, H-8), 7.68 (d, J = 7.9 Hz, 1H, H-3′), 7.51 (t, J = 7.6 Hz, 1H, H-6′), 7.42 (d, J = 7.7 Hz, 1H, H-5′), 7.34 (t, J = 7.6 Hz, 1H, H-4′), 6.87 (dd, J = 2.5, 8.8 Hz, 1H, H-7), 6.69 (d, J = 2.4 Hz, 1H, H-5), 3.88 (s, 3H, OCH_3), 3.80 (m, 1H, H_x), 2.93 (m, 2H, CH_aH_b-Ph), 2.82 (m, 2H, CH_2, H-3), 2.06 (m, 1H, CH_AH_B), 1.86 (m, 1H, CH_AH_B). ^{13}C NMR: δ 197.6 (C, C=O), 163.5 (C, C-6), 146.4 (C), 139.3 (C), 131.7 (CH), 131.6 (CH), 130.0 (CH), 129.3 (C–F), 129.1 (C, C–F), 126.2 (CH), 126.15 (CH), 126.1 (C), 125.7 (C–F), 123.5 (C–F), 113.2 (CH), 112.4 (CH), 55.4 (CH_3), 49.0 (CH, CH_x), 32.3 (CH_2, CH_aH_bPh) 29.4 (CH_2, C-3), 28.2 (CH_2, CH_AH_B). Anal. Calcd. for $C_{19}H_{17}O_2F_3$ (334.337): C, 68.26%, H, 5.12%. Found: C, 68.03%, H, 5.13%.

*4.2.2.2. 2-(2-Ethylbenzyl)-6-methoxy-tetralone (**4c**).* A dark orange syrup was obtained. Yield: 1.49 g (64%), R_f 0.71 (petroleum ether–EtOAc 3:1 v/v); ^{1}H NMR: δ 8.09 (d, J = 8.8 Hz, 1H, H-8), 7.29–7.12 (m, 4H, Ar), 6.87 (dd, J = 2.5, 8.8 Hz, 1H, H-7), 6.70 (d, J = 2.4 Hz, 1H, H-5), 3.88 (s, 3H, OCH_3), 3.69 (dd, J = 3.7, 14.2 Hz, 1H, CH_aH_b-Ph), 2.92 (m, 2H, CH_2, H-3), 2.72 (q, J = 7.4 Hz, 2H, CH_2CH_3) overlapping (m, 1H, H_x), 2.55 (dd, J = 10.5, 14.2 Hz, 1H, CH_aH_b-Ph), 2.12 (m, 1H, CH_AH_B), 1.84 (m, 1H, CH_AH_B), 1.27 (t, J = 7.6 Hz, 3H, CH_2CH_3). ^{13}C NMR: δ 198.2 (C, C=O), 163.5 (C, C-6), 146.5 (C), 142.5 (C), 137.8 (C), 130.2 (CH), 130.0 (CH), 128.6 (CH), 126.5 (CH), 126.4 (C), 126.2 (CH), 113.2 (CH), 112.5 (CH), 55.4 (CH_3), 48.7 (CH, CH_x), 33.7 (CH_2, CH_aH_bPh) 29.3 (CH_2, C-3), 28.0 (CH_2, CH_AH_B), 25.5 (CH_2CH_3), 15.4 (CH_2CH_3). LRMS (EI$^+$) m/z: 295.4 [M + H]$^+$, 294.3 [M]$^+$, 176.3 ([M + H] − [CH_2–Ph–Et])$^+$, 175.31 ([M] − [CH_2–Ph–Et])$^+$, 91.1 [$C_6H_5CH_2$]$^+$, 77.2 [C_6H_5]$^+$. HRMS (ES$^+$): Calc $C_{20}H_{22}O_2$ [M + H]$^+$ 295.1693. Found 295.1695.

*4.2.2.3. 2-(2-Phenethylbenzyl)-6-methoxy-tetralone (**9c**).* A pale orange waxy solid was obtained. Yield: 1.27 g (63%), R_f 0.78 (petroleum ether–EtOAc 4:1 v/v); ^{1}H NMR: δ 8.09 (d, J = 8.8 Hz, 1H, H-8), 7.31–7.20 (m, 9H, Ar), 6.88 (dd, J = 2.3, 8.8 Hz, 1H, H-5), 6.70 (d, J = 2.3 Hz, 1H, H-7), 3.88 (s, 3H, OCH_3), 3.69 (dd, J = 3.0, 13.6 Hz, 1H, CH_aH_b-Ph), 3.05–2.83 (m, 6H, 3 × CH_2), 2.59 (m, 2H, CH_2), 2.11 (m, 1H, CH_AH_B), 1.83 (m, 1H, CH_AH_B). ^{13}C NMR: δ 198.0 (C, C=O), 163.5 (C, C-6), 146.5 (C), 141.8 (C), 136.9 (C), 140.2 (C), 138.1 (C), 130.3 (CH), 130.0 (CH), 129.9 (CH), 129.5 (CH), 129.4 (CH), 129.3 (CH), 127.1 (CH), 126.7 (C), 126.4 (CH), 126.2 (CH), 113.2 (CH), 112.5 (CH), 55.4 (CH_3), 48.8 (CH, CH_x), 37.4 (CH_2), 34.8 (CH_2), 32.4 (CH_2, CH_aH_bPh), 29.3 (CH_2, C-3), 28.1 (CH_2, CH_AH_B). LRMS (EI+) m/z: 371.4.4 [M + H]$^+$, 370.3 [M]$^+$, 176.3 ([M + H] − [CH_2–Ph–Et])$^+$, 175.31 ([M] − [CH_2–Ph–Et])$^+$, 105.3 [$C_6H_5CH_2CH_2$]$^+$, 91.1 [$C_6H_5CH_2$]$^+$, 77.2 [C_6H_5]$^+$. HRMS (ES$^+$): Calc $C_{26}H_{26}O_2$ [M + H]$^+$ 371.2006. Found 371.2004.

*4.2.3. Ethyl 2-(2-bromobenzyl)-6-methoxy-1-oxo-1,2,3,4-tetrahydro-2-naphthalene carboxylate (**6**)*

A mixture of NaH (60% dispersion in mineral oil, 0.45 g, 10.37 mmol), ethyl-6-methoxy-1-tetralone carboxylate (**5**) [20] (2.5 g, 10.0 mmol) in DMF (30 mL) was heated at 60 °C for 1 h. A solution of 2-bromobenzyl bromide (2.67 g, 10.7 mmol) in DMF (10 mL) was added and the reaction heated at 60 °C for a further 8 h. On completion of the reaction, a few drops of H_2O were added and the resulting suspension extracted with Et_2O (3 × 50 mL). The combined organic extracts were washed with brine (50 mL), dried ($MgSO_4$) and concentrated *in vacuo* to give an oily residue. Purification by flash column chromatography (petroleum ether–EtOAc 100:0 v/v increasing to 80:20 v/v) gave the product as a thick yellow oil. Yield: 2.9 g (69%), R_f 0.69 (petroleum ether–EtOAc 3:1 v/v); ^{1}H NMR: δ 8.09 (d, J = 8.8 Hz, 1H, H-8), 7.55 (dd, J = 1.3, 7.9 Hz, 1H, Ar), 7.30 (dd, J = 1.7, 7.6 Hz, 1H, Ar), 7.19 (m, 1H, Ar), 7.06 (m, 1H, Ar), 6.85 (dd, J = 2.5, 8.8 Hz, 1H, H-7), 6.62 (d, J = 2.5 Hz, 1H, H-5), 4.16 (m, 2H, OCH_2CH_3), 3.85 (s, 3H, OCH_3), 3.69 (dd, J = 14.2, 24.4 Hz, C–CH_2–Ar), 3.06 (m, 1H, H-4), 2.78 (m, 1H, H-4), 2.61 (m, 1H, H-3), 2.05 (m, 1H, H-3), 1.17 (t, J = 7.1 Hz, 2H, CH_2CH_3). ^{13}C NMR: δ 193.2 (C=O, C-1), 171.3 (C=O, C-1′), 163.7 (C, C-6), 145.8 (C), 136.9 (C), 132.9 (CH), 132.2 (CH), 130.7 (CH), 128.3 (CH), 127.3 (CH), 125.4 (C), 125.9 (C), 113.5 (CH), 112.3 (CH), 61.6 (CH2, ethyl), 58.7 (C, C-2), 55.4 (CH_3, OCH_3), 38.4 (CH_2, CH_2Ph), 30.1 (CH_2, C-4), 26.5 (CH_2, H-3), 14.0 (CH_3, ethyl). LRMS (CI$^+$) m/z: 419.3 and 417.2 ($^{81/79}$Br) [M + H]$^+$, 339.2 and 337.3 ($^{81/79}$Br) [M − Br]$^+$, 249.2 and 247.2 ($^{81/79}$Br) [M − 2-bromo $C_6H_5CH_2$]$^+$. HRMS (CI+): Calc $C_{21}H_{22}^{79}BrO_4$ [M + H]$^+$ 417.0696. Found 417.0694.

*4.2.4. 2-(2-Bromobenzyl)-6-methoxy-tetralone (**4d**)*

A suspension of tetralone (**6**) (2.6 g, 6.23 mmol), 48% HBr (13.76 mL) and 96% AcOH (11.5 mL) was stirred at 120 °C for 1.5 h. The mixture was cooled to room temperature and diluted with H_2O (5 mL). The reaction mixture was extracted with Et_2O (3 × 50 mL); the combined organic extracts were dried ($MgSO_4$) and concentrated *in vacuo*. Purification by flash column chromatography (petroleum ether–EtOAc 100:0 v/v increasing to 80:20 v/v) gave the 2-(2-bromobenzyl)-6-methoxy-tetralone (**4d**) as the minor product and the demethylated 2-(2-bromobenzyl)-6-hydroxy-tetralone (**4e**) as the major product.

*4.2.5. 2-(2-Bromobenzyl)-6-methoxy-tetralone (**4d**)*

A yellow oil was obtained. Yield: 0.55 g (26%), R_f 0.82 (petroleum ether–EtOAc 3:1 v/v); ^{1}H NMR: δ 8.07 (d, J = 8.8 Hz, 1H, H-8), 7.58 (dd, J = 1.0, 7.9 Hz, 1H, Ar), 7.29 (m, 2H, Ar), 7.11 (m, 1H, Ar), 6.85 (dd, J = 2.5, 8.8 Hz, 1H, H-7), 6.69 (d, J = 2.5 Hz, 1H, H-5), 3.87 (s, 3H, OCH_3), 3.72 (dd, J = 4.4, 13.9 Hz, 1H, CH_aH_b-Ph), 2.90 (m, 2H, CH_2, H-3), 2.87 (m, 1H, H_x), 2.76 (dd, J = 9.5, 13.8 Hz, 1H, CH_aH_b-Ph), 2.08 (m, 1H, CH_AH_B), 1.88 (m, 1H, CH_AH_B). ^{13}C NMR: δ 197.8 (C, C=O), 163.5 (C, C-6), 146.5 (C), 139.9 (C), 133.0 (CH), 131.7 (CH), 130.0 (CH), 127.9 (CH), 127.3 (CH), 126.2 (C), 124.9 (C), 113.2 (CH), 112.5 (CH), 55.4 (CH_3), 47.7 (CH, CH_x), 36.1 (CH_2, CH_aH_b-Ph) 29.3 (CH_2, C-3), 28.1 (CH_2, CH_AH_B). LRMS (CI+) m/z: 347.1 and 345.2 ($^{81/79}$Br) [M + H]$^+$, 267.2 and 265.3 ($^{81/79}$Br) [M − Br]$^+$, 177.4 and 175.3 ($^{81/79}$Br) [M − 2-bromo $C_6H_5CH_2$]$^+$. HRMS (CI$^+$): Calc $C_{18}H_{18}^{79}BrO_2$ [M + H]$^+$ 345.0485. Found 345.0484.

*4.2.6. 2-(2-Bromobenzyl)-6-hydroxy-tetralone (**4e**)*

A white solid was obtained. Yield: 0.8 g (39%), R_f 0.61 (petroleum ether–EtOAc 3:1 v/v); m.p. 171–174 °C; δ 10.32 (s, 1H, OH), 7.78 (d, J = 8.6 Hz, 1H, H-8), 7.58 (d, J = 8.0 Hz, 1H, Ar), 7.32 (m, 2H, Ar), 7.16 (dd, J = 7.0, 7.9 Hz, 1H, Ar), 6.73 (d, J = 8.6 Hz, 1H, H-7), 6.62 (s, 1H, H-5), 3.48 (dd, J = 4.2, 13.8 Hz, 1H, CH_aH_b-Ph), 2.79 (m, 3H, CH_2, H-3 and CH_x), 2.61 (dd, J = 9.8, 13.8 Hz, 1H, CH_aH_b-Ph), 1.87 (m, 1H, CH_AH_B), 1.71 (m, 1H, CH_AH_B).

^{13}C NMR: δ 196.8 (C, C=O), 161.8 (C, C-6), 146.8 (C), 139.2 (C), 132.6 (CH), 131.8 (CH), 129.4 (CH), 128.3 (CH), 127.6 (CH), 124.2 (C), 124.0 (C), 114.3 (CH), 114.0 (CH), 46.6 (CH, CH_x), 35.4 (CH_2, CH_aH_bPh) 28.1 (CH_2, C-3), 27.4 (CH_2, CH_AH_B). Anal. Calcd. for $C_{17}H_{15}BrO_2$ (331.20): C, 61.65%, H, 4.56%. Found: C, 61.59%, H, 4.58%.

*4.2.7. General procedure for the synthesis of (E)-2-(2-aryl/alkylary-benzylidene)- and benzyl-6-methoxy-tetralone derivatives (**8b** and **9b**)*

2 M aqueous Na_2CO_3 (7 mL) was added to a solution of (*E*)-2-(2-bromobenzylidene)-6-methoxy-tetralone (**5**) (2 mmol) in toluene (15 mL), then $Pd(PPh_3)_4$ (0.1 mmol) was added to the mixture.

Arylboronic acid (4 mmol) in ethanol (4 mL) was added to the above mixture and the reaction was refluxed at 100 °C for 5 h. After the reaction was complete, the residual borane was oxidised by the addition of H_2O_2 (30%, 2 mL) at room temperature for 1 h. The crude product was extracted with CH_2Cl_2 (100 mL) and water (3 × 100 mL), then the organic layer was dried ($MgSO_4$) and concentrated *in vacuo*. Purification by flash column chromatography (petroleum ether–EtOAc 100:0 v/v increasing to 90:10 v/v) gave the product, which was recrystallised with EtOH.

*4.2.7.1. (E)-2-(2-(E)-Styrylbenzylidene)-6-methoxy-tetralone (**8b**).* A light brown solid was obtained. Yield: 51%, R_f 0.68 (petroleum ether–EtOAc 4:1 v/v); m.p. 120–122 °C; ^{1}H NMR: δ 8.20 (d, J = 8.7 Hz, 1H, H-8), 8.06 (s, 1H, -C═CH–Ph), 7.76 (d, J = 7.8 Hz, 1H, Ar), 7.51 (d, J = 7.3 Hz, 1H, Ar), 7.41–7.26 (m, 8H, Ar), 7.10 (d, J = 16.1 Hz, 1H, *trans* –CH═CH–), 6.92 (dd, J = 2.5, 8.7 Hz, 1H, H-5), 6.72 (d, J = 2.5 Hz, 1H, H-7), 3.89 (s, 3H, OCH_3), 2.91 (s, 4H, 2× CH_2). ^{13}C NMR: δ 186.6 (C, C═O), 163.7 (C, C-6), 146.1 (C), 147.3 (C), 136.9 (C), 134.8 (C), 134.7 (CH), 130.9 (CH), 130.8 (CH), 129.6 (CH), 128.7 (CH), 128.5 (CH), 127.9 (CH), 127.1 (C), 127.0 (CH), 126.7 (CH), 126.3 (CH), 125.7 (CH), 113.5 (CH), 112.4 (CH), 55.5 (CH_3), 29.6 (CH_2), 27.5 (CH_2). Anal. Calcd. for $C_{26}H_{22}O_2 \cdot 0.2H_2O$ (370.062): C, 84.39%, H, 6.10%. Found: C, 84.57%, H, 6.49%.

*4.2.7.2. 2-(2-(E)-Styrylbenzyl)-6-methoxy-tetralone (**9b**).* A colourless oil was obtained. Yield: 95%, R_f 0.82 (petroleum ether–EtOAc 4:1 v/v); ^{1}H NMR: δ 8.11 (d, J = 8.8 Hz, 1H, H-8), 7.73 (d, J = 7.4 Hz, 1H, Ar), 7.55 (t, J = 7.3 Hz, 1H, Ar), 7.39 (t, J = 7.5 Hz, 1H, Ar), 7.32–7.24 (m, 5H, Ar), 7.07 (d, J = 16.1 Hz, 1H, *trans* –CH═CH–), 6.87 (dd, J = 2.6, 8.8 Hz, 1H, H-5), 6.69 (d, J = 2.5 Hz, 1H, H-7), 3.93 (dd, J = 3.2, 13.6 Hz, 1H, CH_aH_b-Ph), 3.87 (s, 3H, OCH_3), 2.90 (m, 2H, CH_2, H-3), 2.70 (m, 2H, H_x and CH_aH_b-Ph), 2.09 (m, 1H, CH_AH_B), 1.84 (m, 1H, CH_AH_B). ^{13}C NMR: δ 197.9 (C, C═O), 163.5 (C, C-6), 146.6 (C), 138.3 (C), 137.5 (C), 136.4 (C), 126.0 (C), 134.7 (CH), 130.9 (CH), 130.5 (CH), 130.1 (CH), 129.3 (CH), 128.4 (CH), 127.7 (CH), 127.0 (CH), 126.8 (CH), 126.3 (CH), 125.9 (CH), 113.3 (CH), 112.46 (CH), 55.4 (CH_3), 48.8 (CH, C-2), 33.45 (CH_2), 29.2 (CH_2), 28.0 (CH_2). LRMS (CI^+) m/z: 369.3 $[M + H]^+$, 177.2 $[M - \{6\text{-methoxy-1-tetralone}\}]^+$. HRMS (EI): Calcd. $C_{26}H_{25}O_2$ $[M + H]^+$ 369.1849. Found 369.1843.

4.3. Docking studies

All molecular modelling studies were performed on a MacPro dual 2.66 GHz Xeon running Ubuntu 8. Docking simulations were performed using PLANTS [13] and the results were visualised in MOE [16]. Ligand structures were built in MOE minimised using the MMFF94x forcefield until a RMSD gradient of 0.05 kcal mol^{-1} Å^{-1} was reached. The resulting structures were used in the docking simulations. PLANTS software was used with the default settings (aco_ants 20; aco_evap 0.15; aco_sigma 5.0), defining the binding site as a sphere of 12 Å around the alpha carbon of Ile242. Docking results were imported in a MOE database and examined using the ligand interaction function.

Acknowledgments

For ASA we acknowledge the Embassy of the Arab Republic of Egypt for the award of a PhD scholarship. We also acknowledge the EPSRC Mass Spectrometry Centre, Swansea, UK for mass spectroscopy data.

References

[1] G. Jones, S.A. Strugnell, H.F. DeLuca, Physiol. Rev. 78 (1998) 1193–1231.
[2] S. Masuda, G. Jones, Mol. Cancer Ther. 5 (2006) 797–808.
[3] D.E. Prosser, G. Jones, Trends Biochem. Sci. 29 (2004) 664–673.
[4] I. Schuster, H. Egger, P. Nussbaumer, R.T. Kroemer, J. Cell. Biochem. 88 (2003) 372–380.
[5] M. Kahraman, S. Sinishtaj, P.M. Dolan, T.W. Kensler, S. Peleg, U. Saha, S.S. Chuang, G. Bernstein, B. Korczak, G.H. Posner, J. Med. Chem. 47 (2004) 6854–6863.
[6] S.W. Yee, M.J. Campbell, C. Simons, J. Steroid Biochem. Mol. Biol. 98 (2006) 228–235.
[7] S. Swami, A.V. Krishnan, D.M. Peehl, D. Feldman, Mol. Cell. Endocrinol. 241 (2005) 49–61.
[8] S.W. Yee, C. Simons, Bioorg. Med. Chem. Lett. 14 (2004) 5651–5654.
[9] G.A. Wachter, R.W. Hartmann, T. Sergejew, G.L. Grun, D. Ledergerber, J. Med. Chem. 39 (1996) 834–841.
[10] G.H. Posner, K.R. Crawford, H.W. Yang, M. Kahraman, H.B. Jeon, H. Li, J.K. Lee, B.C. Suh, M.A. Hatcher, T. Labonte, A. Usera, P.M. Dolan, T.W. Kensler, S. Peleg, G. Jones, A. Zhang, B. Korczak, U. Saha, S.S. Chuang, J. Steroid Biochem. Mol. Biol. 89–90 (2004) 5–12.
[11] A.J. Kirby, R. LeLain, P. Mason, F. Maharbouie, P.J. Nicholls, H.J. Smith, C. Simons, J. Enz. Inhib. Med. Chem. 18 (2003) 27–33.
[12] W.S. Rapson, R.G.J. Shuttleworth, J. Chem. Soc. (1940) 636–641.
[13] T. Weskamp, V.P.W. Bohm, W.A. Herrmann, J. Organomet. Chem. 585 (1999) 348–352.
[14] O. Korb, T. Stützle, T.E. Exner, Swarm Intell. 1 (2007) 115–134.
[15] M.S. Gomaa, C. Simons, A. Brancale, J. Steroid Biochem. Mol. Biol. 104 (2007) 53–60.
[16] G. Jones, V. Byford, S. West, S. Masuda, G. Ibrahim, M. Kaufmann, J. Knutson, S. Strugnell, R. Mehta, Anticancer Res. 26 (2006) 2589–2596.
[17] Molecular Operating Environment 2008.10 (MOE).http://www.chemcomp.com.
[18] D.D. Perrin, W.L.F. Armarengo, Purification of Laboratory Chemicals, third ed. Pergamon Press, New York, 1988.
[19] S.W. Yee, L. Jarno, M.S. Gomaa, C. Elford, L.-L. Ooi, M.P. Coogan, R. McClelland, R.I. Nicholson, B.A.J. Evans, A. Brancale, C. Simons, J. Med. Chem. 48 (2005) 7123–7131.
[20] B.T. Cho, S.K. Kang, S.H. Shin, Tetrahedron: Asymmetry 13 (2002) 1209–1217.